Harmonic generation in paramagnetic spin systems

Article · June 1983

CITATIONS
0

READS
23

2 authors, including:

Thomas A Detemple
University of Illinois, Urbana-Champaign
120 PUBLICATIONS **2,044** CITATIONS

SEE PROFILE

UILU-ENG-83-2545

Harmonic Generation in Paramagnetic Spin Systems

Prepared by
M. K. Gurnick and T. A. DeTemple
Department of Electrical Engineering
University of Illinois
Urbana, IL 61801

June 1983

Contract DAAG 29-81-K-0175
Final Report for the Period October 1, 1981 - April 1, 1983

Prepared for
Dr. Robert Guenther
U. S. Army Research Office
P. O. Box 12211
Research Triangle Park, NC 27709

UNCLASSIFIED

SECURITY CLASSIFICATION OF THIS PAGE (When Data Entered)

REPORT DOCUMENTATION PAGE		READ INSTRUCTIONS BEFORE COMPLETING FORM
1. REPORT NUMBER	2. GOVT ACCESSION NO.	3. RECIPIENT'S CATALOG NUMBER
4. TITLE (and Subtitle) Harmonic Generation in Paramagnetic Spin Systems		5. TYPE OF REPORT & PERIOD COVERED Final 10-1-81/4-1-83 6. PERFORMING ORG. REPORT NUMBER UILU-ENG-83-2545
7. AUTHOR(s) T. A. DeTemple M. K. Gurnick		8. CONTRACT OR GRANT NUMBER(s) DAAG29-81-K-0175
9. PERFORMING ORGANIZATION NAME AND ADDRESS University of Illinois Department of Electrical Engineering Urbana, IL 61801		10. PROGRAM ELEMENT, PROJECT, TASK AREA & WORK UNIT NUMBERS
11. CONTROLLING OFFICE NAME AND ADDRESS U. S. Army Research Office Post Office Box 12211 Research Triangle Park, NC 27709		12. REPORT DATE June 1983 13. NUMBER OF PAGES 34
14. MONITORING AGENCY NAME & ADDRESS(if different from Controlling Office)		15. SECURITY CLASS. (of this report) Unclassified 15a. DECLASSIFICATION/DOWNGRADING SCHEDULE

16. DISTRIBUTION STATEMENT (of this Report)

Approved for public release; distribution unlimited.

17. DISTRIBUTION STATEMENT (of the abstract entered in Block 20, if different from Report)

NA

18. SUPPLEMENTARY NOTES

The view, opinions, and/or findings contained in this report are those of the author(s) and should not be construed as an official department of the Army position, policy, or decision unless so designated by other documentation.

19. KEY WORDS (Continue on reverse side if necessary and identify by block number)

Second harmonic generation
Paramagnetic spin systems
superlattice
Third harmonic generation

20. ABSTRACT (Continue on reverse side if necessary and identify by block number)

The theory of resonant second and third harmonic generation is considered and applied to the case of paramagnetic spin systems tuned by a magnetic field. Using available spectroscopic and material parameters, conversion efficiencies of around 25% seem feasible. Optical nonlinearities in semiconductor superlattice are considered and shown to have large second order optical nonlinearities in the mid-infrared.

DD FORM 1 JAN 73 1473 EDITION OF 1 NOV 65 IS OBSOLETE

UNCLASSIFIED

SECURITY CLASSIFICATION OF THIS PAGE (When Data Entered)

TABLE OF CONTENTS

I. Introduction

This report summarizes the research performed under DAAG-29-81-K-0175. The objectives of the research were to assess the merits of resonant frequency doubling in paramagnetic spin systems in the near millimeter (NMM) region. The motivation for this occurs because the efficiency of conventional solid state devices falls as ω^{-2} so that a doubler with a conversion efficiency of > 25% would have a higher system efficiency at 2ω than a primed power source.

In Sections II and III we review the main characteristics of resonant frequency doubling from an optical standpoint in a three-level system. In Section IV we consider the characteristics of available spin ions in candidate host materials and show that the approach does not seem promising because of inordinately long crystal lengths. In Section V we comment on resonant frequency tripling in a three-level system and in Section VI we comment on the possibilities which might exist in heterostructure super-lattices.

II. Overview

In an earlier paper[1] a semiclassical treatment of second harmonic generation in a three-level system was considered, motivated by recent experimental observations of doubling in iron doped rutile in the microwave.[2] A density matrix description of three-wave parametric interactions was used to obtain analytical nonperturbative solutions for the nonlinear polarization within the limits of the rotating wave approximation, RWA. In Fig. 1 the perturbation results are presented for the second harmonic polarization in a three-level system with and without the RWA. Clearly, this is an excellent approximation for the nearly resonant and resonant cases.

The nonlinear polarizations were next coupled with Maxwell's equations and solved numerically. For a strongly saturating pump and for certain matrix elements, large conversion efficiencies ($> 50\%$) were predicted. These results were ascribed to the large nonlinear polarization associated with a resonant system and to AC Stark splitting of the harmonic transition for $\Lambda_{23} >> \Lambda_{12}$ which minimizes absorption of the harmonic. Additionally the pump decay is linear with distance.

In this report we first expand on the results presented earlier for harmonic generation in a three-level system and then we apply these results to magnetic resonance systems. Clogston[3] was the first to treat this problem albeit in the limit of a strong pump and a weak harmonic. Related are calculations of frequency conversion in a four-level system again in the strong

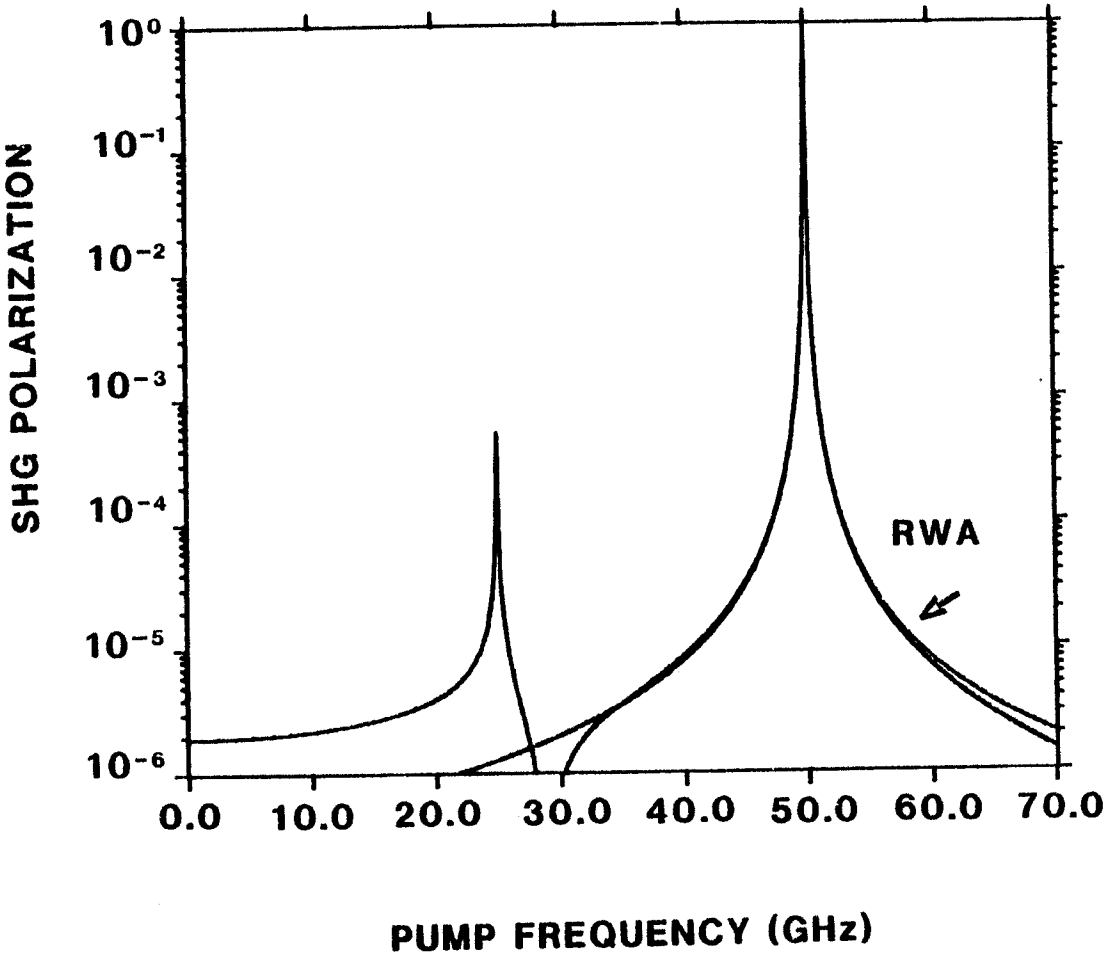

Figure 1. Perturbation calculation of SHG polarization with and without the rotating wave approximation. $\Omega_{12} = \Omega_{23} = 50$ GHz.

pump limit,[4] and calculations of harmonic generation in two level spin systems[5,6] and in fully nonresonant systems.[7]

In addition, many authors have reported experimental observation of nonlinear effects in paramagnetic materials. Kellington[8] was the first to observe second harmonic generation from ruby crystals at room temperature. Boscaino, et al.[5,6,9] extended this work to include low temperatures and saturation effects. A number of other experiments have been reported in resonant[10,11,2] and either nonresonant or two-photon resonant systems.[12,13] The best conversion efficiency (10^{-4}) was obtained by Yngvesson and Kollberg[2] in Fe^{+3}/rutile at liquid helium temperature for the fully resonant case. Encouraged by these results, we calculate the practical limits of resonant second harmonic in this system.

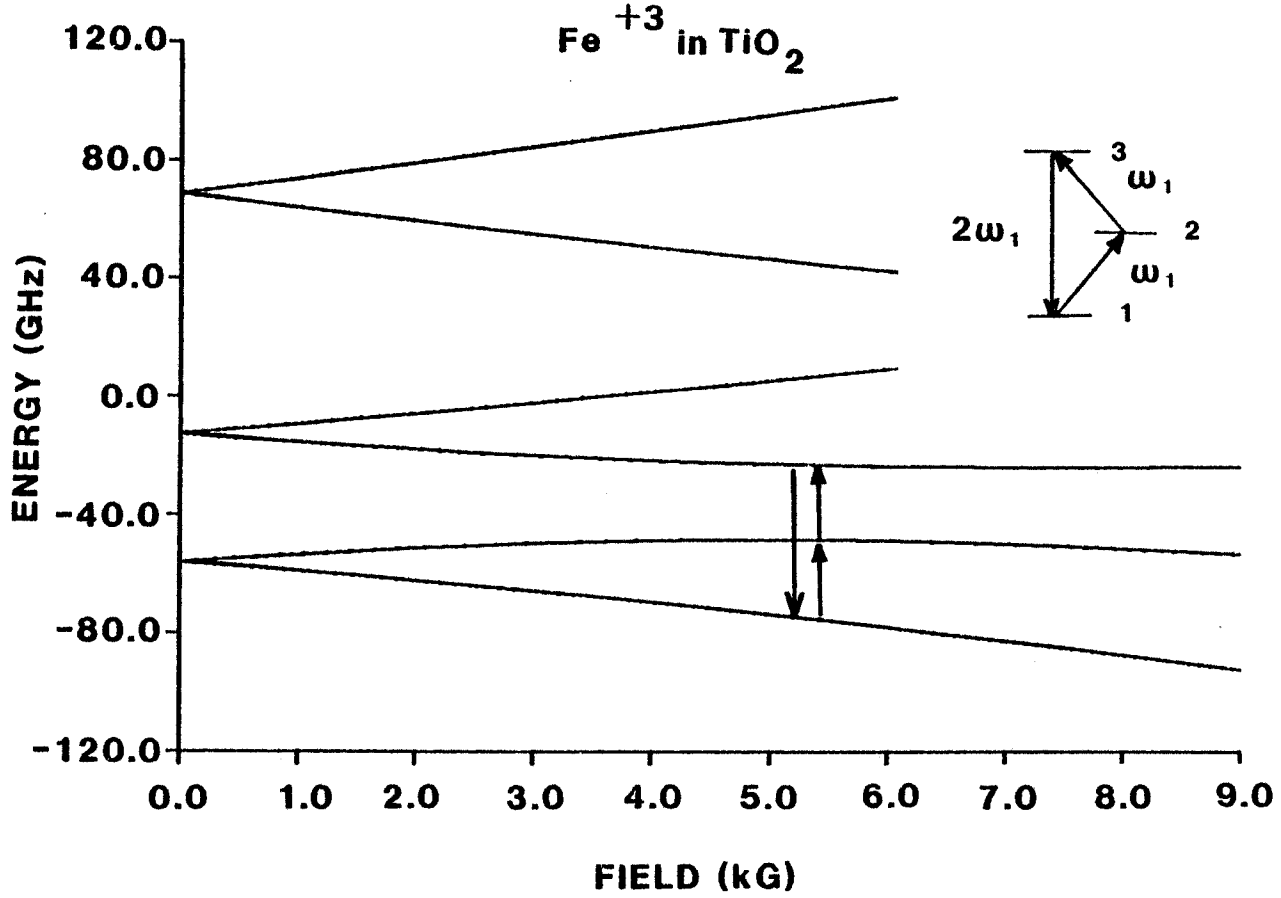

Figure 2. An energy level diagram for Fe^{+3} in rutile at an angle 45° from either a axis and 32.5° from the a, a plane. Spin Hamiltonian parameters are from Carter and Okaya.[22]

III. General Considerations

a) Basic Equations

In this section some definitions and results presented in an earlier paper[1] and relevant to the following are reviewed.

The initial growth of the harmonic intensity accompanying the linear decay of a saturating pump was shown to be

$$I_H = \frac{2}{R_\gamma}\left\{\frac{R_\gamma|\rho_{13}^a|\zeta}{\Lambda_{12}(0)}\right\}^2 \tag{1}$$

where $R_\gamma = k_3|\vec{\mu}_{13}\cdot\varepsilon_3|^2/k_1|\vec{\mu}_{12}\cdot\varepsilon_1|^2$, $\Lambda_{12} = \vec{\mu}_{12}\cdot\vec{E}_1 e^{i\theta/2\hbar}$, ζ is a dimensionless space variable and ρ_{13}^a is the parametric contribution to the second harmonic intensity. The latter, again in the strong pump limit,can be written as a function of the saturated population differences,which may be positive, negative or even zero, or

$$\rho_{13}^a = \frac{\Lambda_{12}\Lambda_{23}}{L_{13}^a}\left[\frac{(\rho_{11}-\rho_{22})}{L_{12}^a} - \frac{(\rho_{22}-\rho_{33})}{L_{23}^a}\right] \times \frac{1}{\left[1 - \frac{\Lambda_{23}^2}{L_{12}^a L_{13}^a} - \frac{\Lambda_{12}^2}{L_{13}^a L_{23}^a}\right]} \tag{2}$$

where ρ_{11}, ρ_{22}, ρ_{33} represent level populations and $L_{13}^a = \Omega_{13} + \omega_3 - i/\tau_{13}$, $L_{12}^a = \Omega_{12} + \omega_1 - i/\tau_{12}$, and $L_{23}^a = \Omega_{23} + \omega_2 - i/\tau_{23}$ are the complex detunings. ζ, the space variable, is related to an actual propagation distance by the line center Beer's coefficient, α_{12}, for the $|1> \rightarrow |2>$ transition. $\zeta T_2 = \alpha_{12}\, z/2$ therefore, if the

Rabi frequencies are expressed in units of T_2, ζ measures the distance in units of field Beer's coefficient. The harmonic intensity is normalized to the pump intensity by defining

$$I_H = \frac{2}{R_\gamma}\left[\frac{|\Lambda_{23}(\zeta)|^2}{\Lambda_{12}(0)}\right] = \frac{|\vec{E}_3(\zeta)|^2}{|\vec{E}_1(0)|^2} \tag{3}$$

b) Temperature Dependence

A particularly simple limit for ρ_{13}^a is arrived at when $T_1=T_2$ and all matrix elements are equal.[1] Then

$$\rho_{13}^a = -\frac{1}{8}\left\{(\rho_{11}^e-\rho_{22}^e) - (\rho_{22}^e-\rho_{33}^e)\right\} \tag{4}$$

which implies an interference effect as $|2\rangle$ is populated and hence a decrease in the value of ρ_{13}^a with an increase in temperature. Therefore, from Eq. (1) the initial growth of the harmonic intensity requires a larger conversion distance. No significant change in the peak conversion efficiency is predicted in a three-level system, however, if other nearby levels are populated a reduction in the harmonic intensity would be expected. In Fig. 3 the peak conversion efficiency and distance are plotted for $T_1=T_2$ and T_1 = 100 T_2 for $\Lambda_{12}T_2$ = 4 and R_μ = 6. In each case for $\Delta E/kT \gg 1$ the conversion distance is observed to increase sharply with temperature. No significant change in the peak efficiency is predicted.

c) $T_1 \neq T_2$

The effect of $T_1 \neq T_2$ can be qualitatively predicted from the T_1 dependence of the population terms.[14]

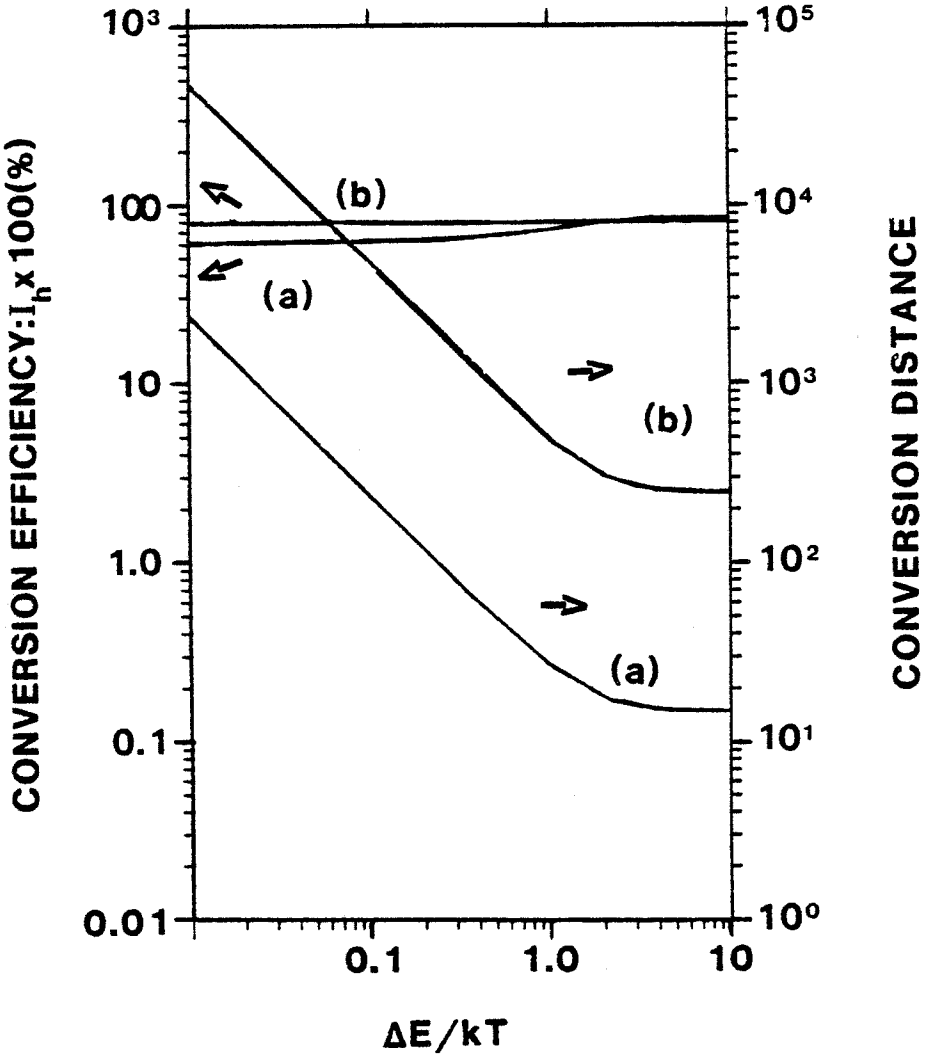

Figure 3. Conversion efficiency and conversion distance (in relative units) as a function of temperature for R_μ=6, $T_2\Lambda_{12}$=4 and (a) T_1=T_2 and (b) T_1=100×T_2.

$$(\rho_{22}-\rho_{11}) = -\frac{(1 + 2T_1B-T_1)}{1 + 2T_1(A+B-a) + 3T_1^2(AB-c^2)} \tag{5a}$$

and

$$(\rho_{33}-\rho_{11}) = \frac{2T_{1a}}{1 + 2T_1(A+B-a) + BT_1^2(AB-a^2)} \tag{5b}$$

where $A = \frac{2\Lambda_{12}(1+\Lambda_{12}^2)}{1 + (\beta^2+1)\Lambda_{12}^2}$ $\qquad a = \frac{2R_\mu^2\Lambda_{12}^4}{1 + (R_\mu^2+1)\Lambda_{12}^2}$

$$B = \frac{2R_\mu^2\Lambda_{12}^2(1 + R_\mu L_{12}^2}{1 + (R_\mu^2+1)\Lambda_{12}^2} \qquad R_\mu = \frac{\hat{\varepsilon}_1\cdot\vec{\mu}_{23}}{\hat{\varepsilon}_1\cdot\vec{\mu}_{12}}$$

These equations are derived by considering the population equations for a resonant field and a negligible Λ_{13}. With an increase in T_1 the population differences decrease and therefore saturation occurs more quickly, the pump decay is slower and from Eq. (1) the build up of the harmonic is slower and more spread out. Figures 4 and 5 are plots of maximum conversion efficiency and distance for several T_1/T_2 ratios and a variety of matrix element ratios. The conversion distance is predicted to increase sharply while little change in peak conversion efficiency is expected. Previously, for $T_1=T_2$ a resonance was observed for $R_\mu = 1/\sqrt{2}$. A similar resonance is not calculated when $T_1 \neq T_2$.

d) Variation of Individual Transition Probabilities

Transition probabilities between different pairs can differ significantly depending on the forbiddance of the transition between states and on the degree of mixing of states. The

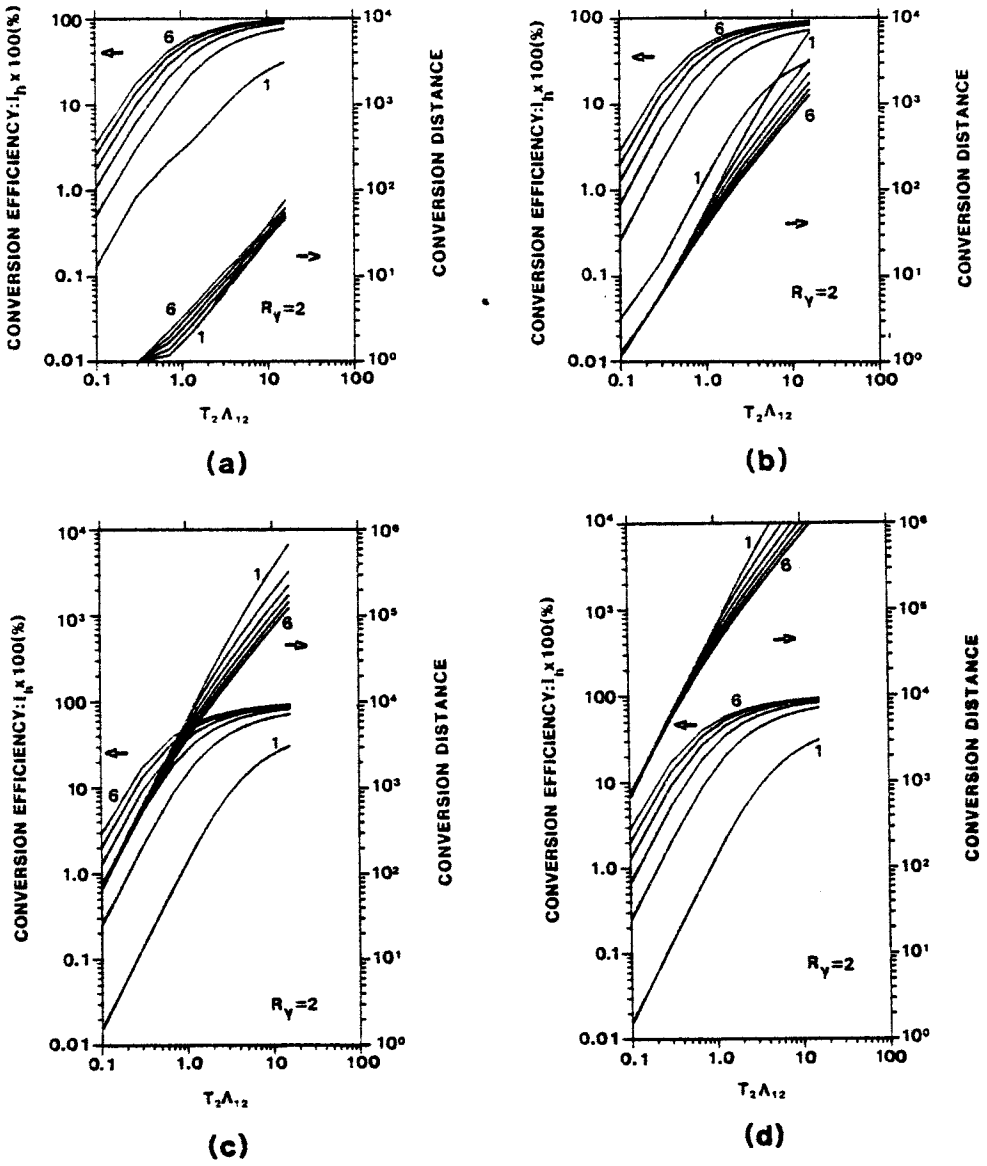

Figure 4. Conversion efficiencies and conversion distances (in relative units) as a function of $\Lambda_{12}T_2$ for x=y=z=0 R_μ=1-6, ρ^e_{11}=1 and for (a) $T_1=T_2$, (b) $T_1=100T_2$, (c) $T_1=10^{-4}T_2$, and (d) $T_1=10^{-5}T_2$.

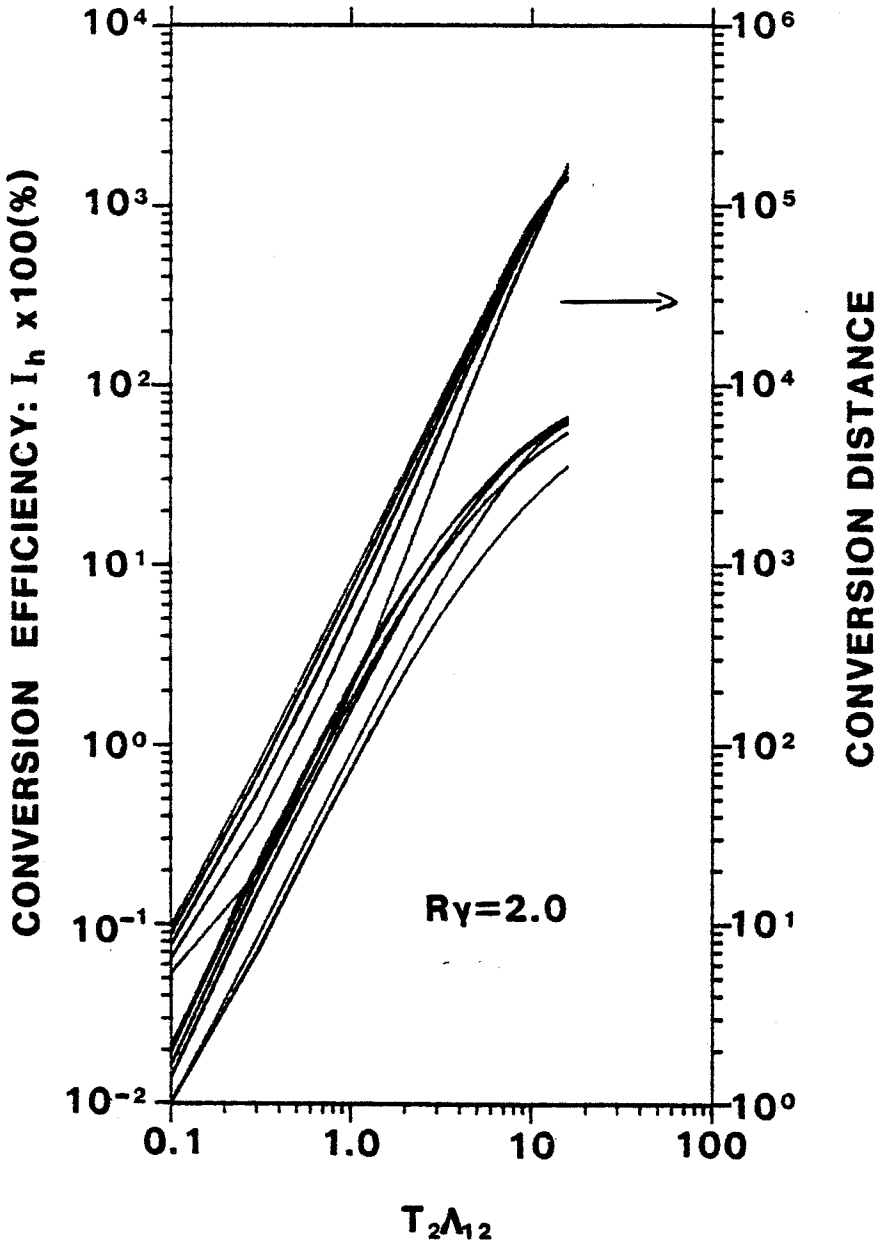

Figure 5. Conversion efficiencies and conversion distances (in relative units) as a function of $\Lambda_{12}T_2$ for x=y=z=0 R_μ=.25-1.25 (increments of .25) for $T_1=1\times10^{-3}T_2$.

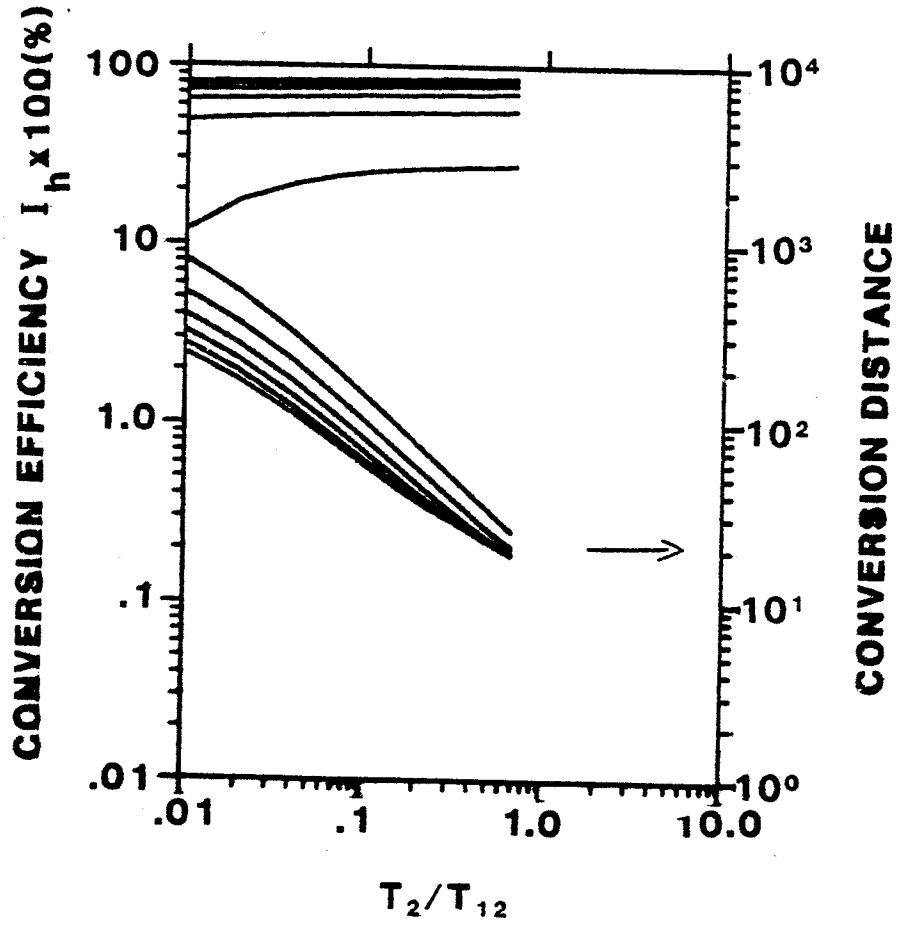

Figure 6. Variation of conversion efficiencies and conversion distances (in relative units) with T_2/T_{12}. $T_{13} = T_{23} = 100 \times T_2$, x=y=x=0, ρ^e_{11}=1 and R_μ = 1-6.

general form of the population equations can be written[3]

$$\dot{\rho}_{jj} = [H',\rho]_{jj} + \sum_{k} (\rho_{kk}\omega_{kj} - \rho_{ii}\omega_{jk}) \qquad (6)$$

where ω_{kj} is a per unit time transition probability subject to the constraints of detailed balancing. A relaxation time can be defined as $T_{ji} = T_{ij} = \frac{1}{\omega_{ij}} \dot{\rho}_{ij}$. In Figs. 6 and 7 we show the effect on the conversion distance of decreasing respectively T_{12} and T_{13} from $100\times T_2$ to T_2. All other T_{ij} are set equal to $100\times T_2$. In each case as T_{12} or T_{13} approach T_2 the conversion distance approaches that calculated for a decrease in the overall T_1. However, a decrease in T_{23} does not significantly affect the conversion distance as is expected considering the interference effect associated with populating $|2\rangle$.

e) Effect of Detuning

In Figs. 8, 9, and 10 the conversion efficiency and conversion distance are plotted versus $\Lambda_{12}T_2$ for a system where the pump is detuned by 10 linewidths and the harmonic is resonant and for the case where the pump is detuned by 10 linewidths and the harmonic is detuned by 20 linewidths. In each case a decrease in the conversion efficiency is predicted as well as in increase in the conversion distance. Both the conversion efficiency and conversion distance converge to the resonant case as the line is power-broadened.

These results are consistent with the non-zero absorption which is observed when the system is not on one and two-photon resonance.[1]

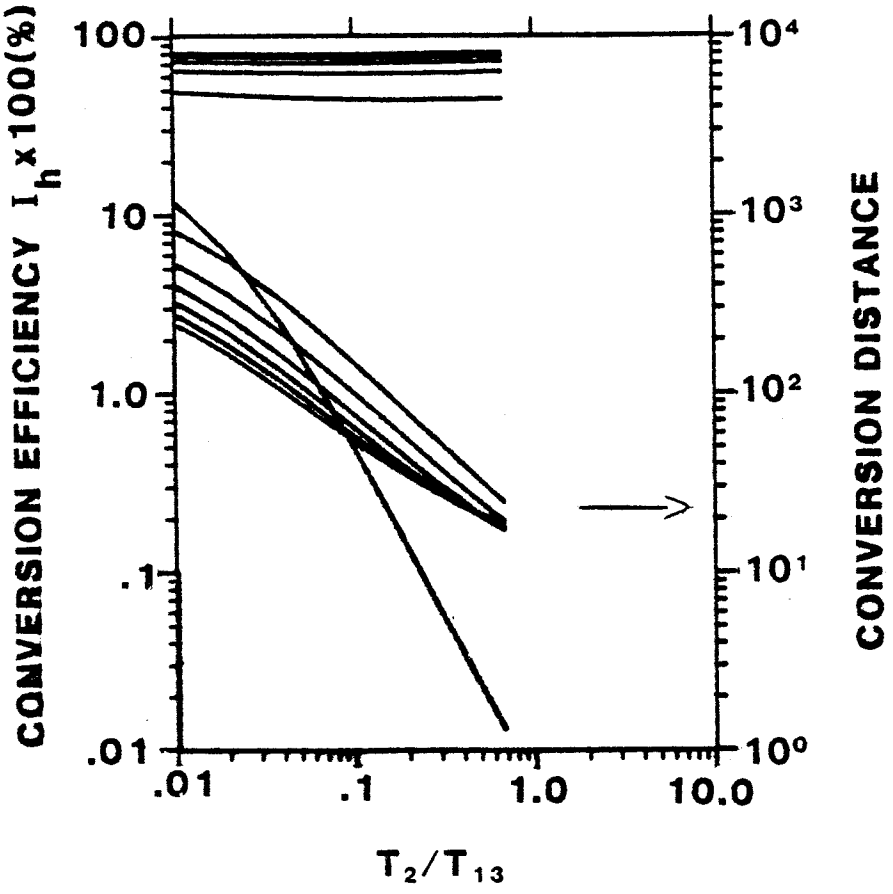

Figure 7. Variation of conversion efficiencies and conversion distances (in relative units) with $T_{12} = T_{23} = 100 \times T_2$, x=y=z=0, $\rho^e_{11} = 1$ and $R_\mu = 1\text{-}6$.

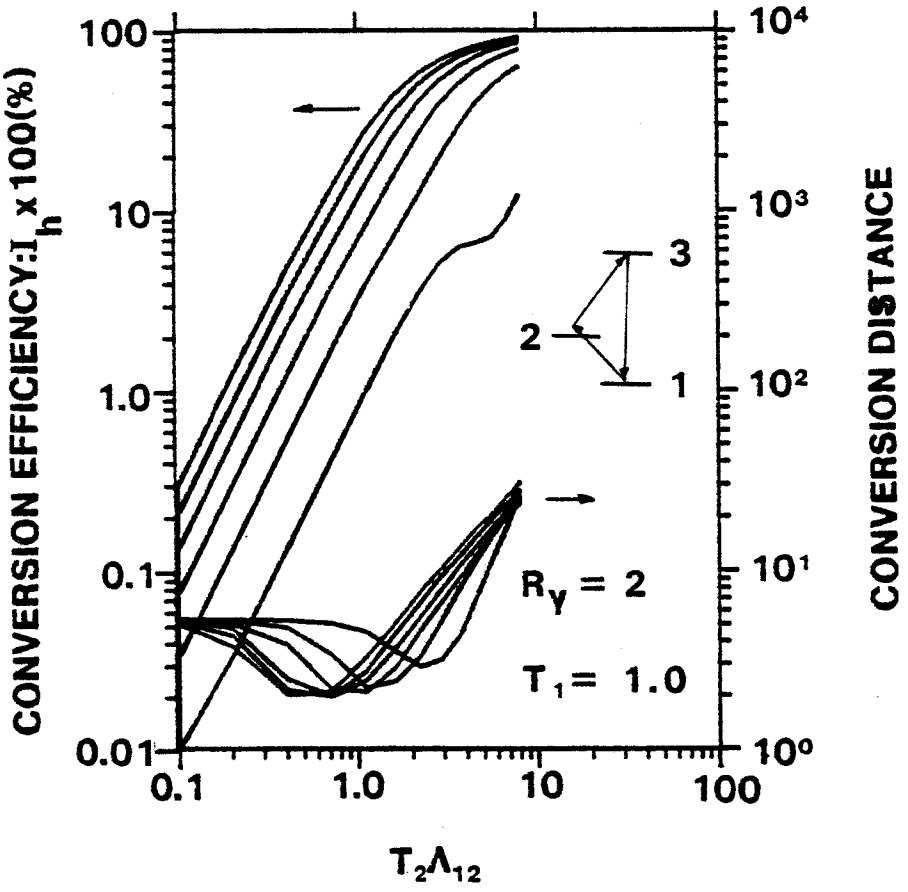

Figure 8. Plot of conversion efficiencies and conversion distances (in relative units) for x=-y=10, z=0, $\rho^e_{11} = 1$ and $R_\mu = 1\text{-}6$. $T_1 = T_2$.

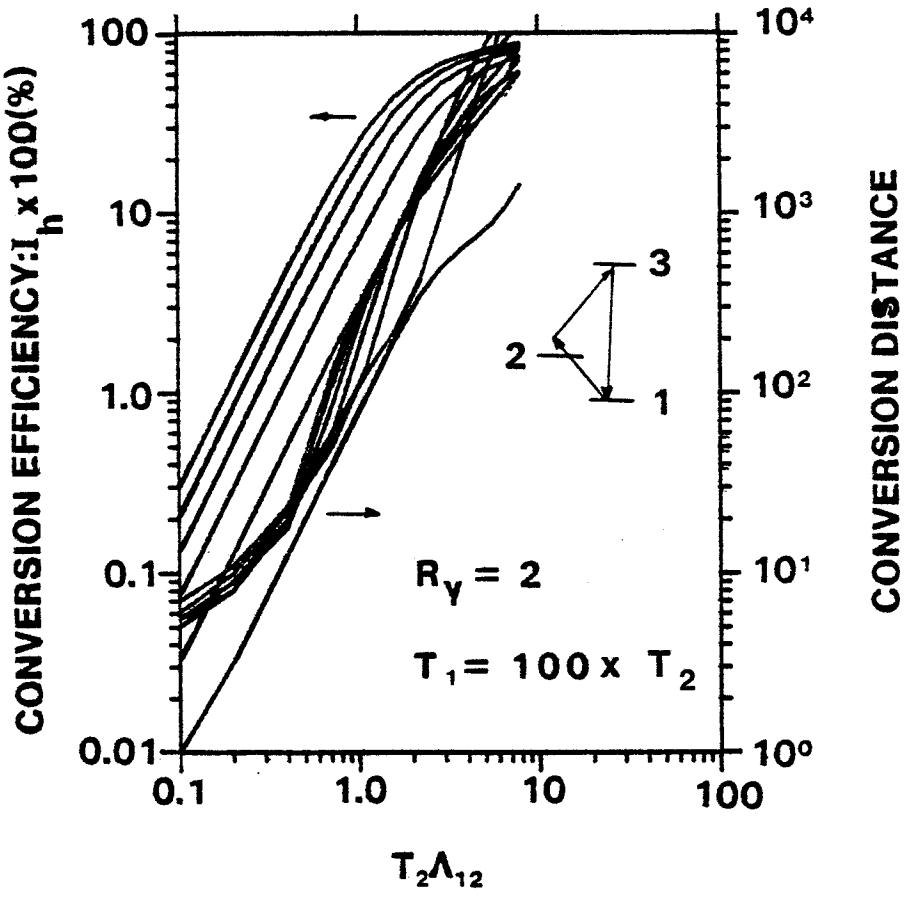

Figure 9. Plot of conversion efficiencies and conversion distances (in relative units for x=-y=10 and z=0, $\rho^e_{11} = 1$ and $R_\mu = 1\text{-}6$. $T_1 = 100 \times T_2$.

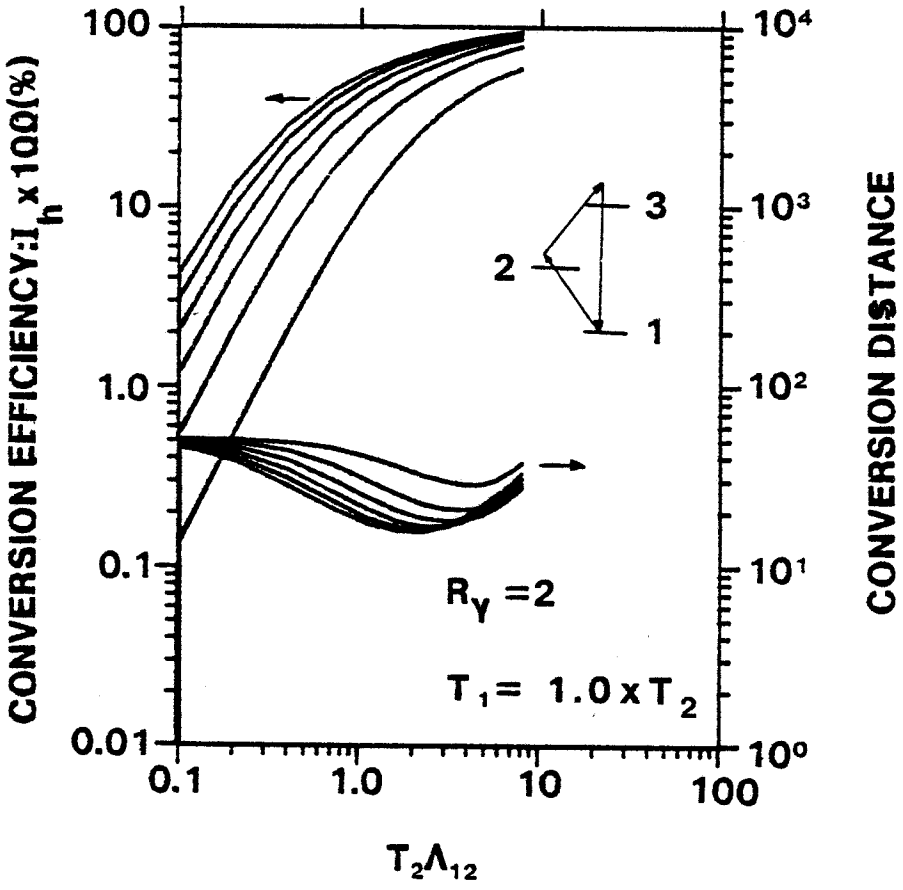

Figure 10. Plot of conversion efficinecies and conversion distances (in relative units) for x=y=10, z=20, ρ^e_{11} = 1 and R_μ = 1-6.

f) Effect of Inhomogeneous Line Broadening

A treatment of inhomogeneous line broadening follows directly from the consideration of detuning in the previous section. If we consider a system with a Gaussian distribution of detunings, for example, the velocity distribution in a Doppler broadened line, then the total nonlinear polarization is the sum of the nonlinear polarization associated with each velocity point (detuning). In Figs. 11 a) and b) peak conversion efficiencies and conversion distances are plotted for several T_1/T_2 ratios and a variety of inhomogeneous linewidths. As expected for inhomogeneous linewidths which are larger than T_2 the loss in conversion efficiency is significant (> 25%) as is the increase in conversion distance. Again the results converge to the homogeneous case as the line is power broadened. In general, as for the homogeneous case, the larger matrix elements result in the best conversion efficiencies.

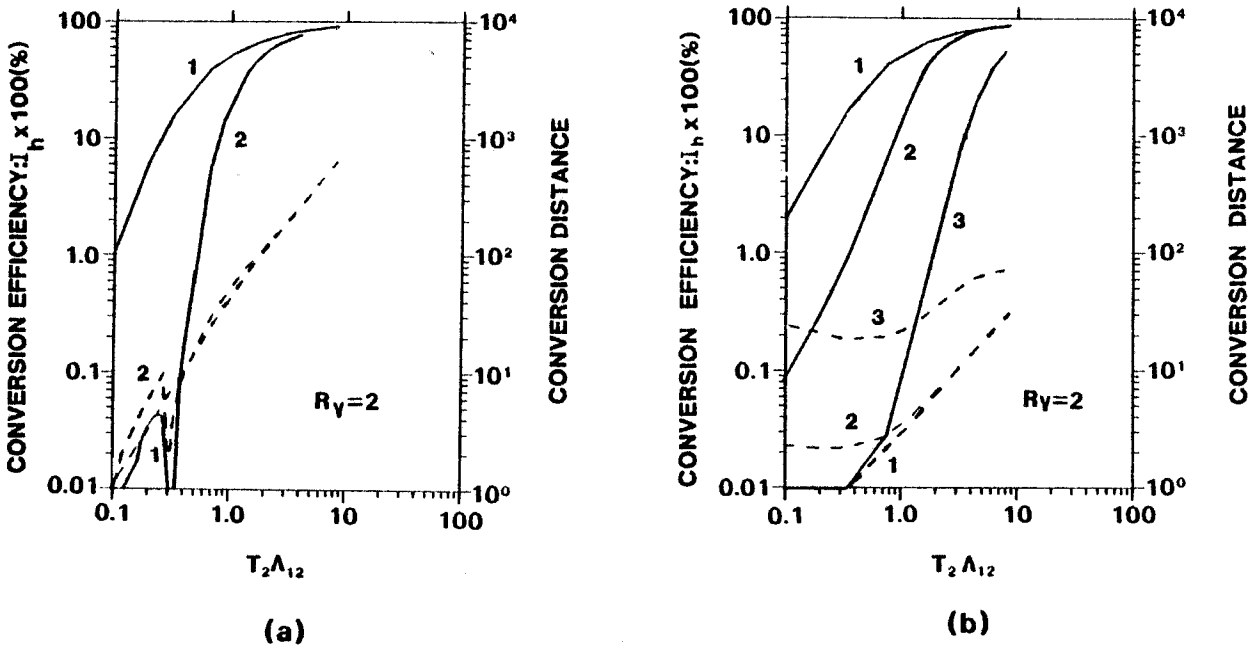

Figure 11. Conversion efficiencies and conversion distance (in relative units) including inhomogeneous line broadening as a function of $\Lambda_{12}T_2$ for x=y=z=0, R_μ=6, ρ_{11} = 1 and for (a) T_1=100T_2 and (b) T_1=T_2. (1) T_2^* = T_2, (2) T_2^* = 10T_2, and (3) T_2^* = 100 T_2.

IV. Application to Magnetic Resonance Systems

Encouraged by the report of Yngvesson and Kollberg[2] of efficient second harmonic generation in iron doped rutile we have calculated the practical limits of conversion efficiency in this and similar paramagnetic materials. Materials which exhibit nuclear magnetic resonance are not considered since the moments are a thousand times less and the energy level splitting are much smaller.[15]

Iron doped rutile is a convenient system to use as a model since much is known about its magnetic resonance and material properties due to an earlier interest in maser materials.[16,17-19] In addition it is representative of a large group of paramagnetic compounds the transition metals and the loss tangent is relatively small ($\geq 10^{-5}$). In rutile, the Fe^{+3} ion is situated at two magnetically inequivalent sites of D_{2h} symmetry which are related to each other and to the optic axis by a rotation of 90°. The spin Hamiltonian is characteristic of an ion (s=5/2) at a site of tetragonal symmetry.[20,21] The spin Hamiltonian parameters have been shown to be:[22]

D = 20.35 GHz	E = 2.21±0.07 GHz
a = 1.1 to 0.6 GHz	F = -0.5±0.3 GHz

Inasmuch as the zero field splitting is large, substantial energy level splittings are obtainable with small magnetic fields. Spectra of the two inequivalent sites coincide in a plane defined by the c-axis. Figure 2 is an energy level diagram for Fe^{+3} in rutile at

an angle 45° from an a-axis and 32.5°from the a-a plane. A possible parametric interaction is indicated. In this system at a concentration of 1×10^{20} cm^{-3} and an estimated T_2 of 1×10^{-8} sec, the scale factor, $\alpha_{12/2}$, is approximately 15 cm^{-1} at a frequency of 3 cm^{-1}. It should be noted that concentrations of this order of magnitude are unrealistic in rutile[23] although realizable in hosts (spinels, corundum, etc.) where problems with charge compensation do not occur.

The longitudinal, T_1, relaxation properties of Fe^{+3} doped rutile are well characterized.[24-28,29,30] Above 10°K T_1 is dominated by Raman-type processes and at room temperatures the relaxation time is controlled by direct processes and is on the order of a few milliseconds.[25] This is roughly four to five orders of magnitude larger than T_2. Neglecting for the moment inhomogeneous line broadening and assuming only the ground state to be populated, Fig. 4 d) is representative of Fe^{+3}/rutile at liquid helium temperatures. From this plot and considering a scale factor of 15 cm^{-1} we see that for conversion efficiencies on the order of 25% or better the crystal would need to be roughly a thousand centimeters in length. From Fig. 3 we see that a further increase in conversion distance is expected if we consider that $\Delta E/kT \sim 1$ and therefore approximately one-third of the total population is not in the ground state.

Apparently, in order to achieve realistic conversion distances, T_1 must be decreased relative to T_2. At room tempeature T_1

approaches T_2 but all levels become almost equally populated. Referring again to Fig. 3 for $\Delta E/kT = .01$ and $T_1=T_2$ a hundred centimeter crystal would be required. Another possibility is to exploit nonresonant and resonant cross-relaxation processes between Fe^{+3} and faster relaxing ions. Cross-relaxation has been extensively investigated in ruby and is attributed to magnetic dipole and virtual phonon interactions as well as quadrapole electric field effects.[31-33] Of course, the maximum decrease in T_1 is observed for resonant processes where an impurity would contribute pump absorption. T_1 can also be decreased by increasing the concentration of ions in the host.[27] This is probably related to an increase in exchange interactions. The conversion distance can also be decreased by increasing T_2. It has been shown[34,5,6,9,35] that when the oscillating magnetic field is much larger than the local field seen by each ion, T_2 can be effectively reduced for the pump transition. This has been demonstrated in ruby and DPPH,[5,6,36] and more recently for an optical transition in $Pr:LaF_3$.[52] In the former case, T_1 was reduced to 10^{-7} sec. It is limited by local fields with a finite correlation time.[35] In ruby the upper limit on T_2 is determined by surrounding ^{27}Al ions[6] (I=5/2) of the host lattice. In rutile roughly 90% of the titanium sites are occupied by isotopes with I=0. Therefore, a somewhat longer T_2 might be realized. In addition an anomolously low T_2 has been observed for transitions close to the zero field splitting.[37,38] It is also important to remember that increasing T_2 also increases the scale factor hence further reducing the actual material length.

If, in fact T_1 can be made roughly equal to T_2 and T_2 can be reduced to 10^{-6}-10^{-7} sec substantial conversion efficiencies at moderate conversion distance might be feasible. As an example, for $T_2=T_1=1\times10^{-7}$ sec the scale factor, assuming a concentration of 1×10^{20} cm^{-3} is 150 cm^{-1}. For $\Lambda_{12}T_2 = 10$ the conversion distance is on the order of 0.2 cm and for certain combinations of matrix elements will approach 100%.

Of course random crystal defects and impurities will result in local field variations from site to site in the host.[39] Therefore, the linewidths of magnetic resonance systems are usually inhomogeneously broadened with T_2^* varying from 10^{-7}-10^{-9} sec. This effect enters into the calculation in two ways. First, the scale factor is now calculated from T_2^*, the inhomogeneous linewidth. Second, a spin system must now be considered where each individual spin packet is not on resonance but rather a Gaussian distribution about full resonance is assumed.

Linewidths observed for iron-doped rutile at high concentrations (1×10^{19} cm^{-3}) are very broad, several hundred Gauss at x-band frequencies[23] corresponding to a T_2^* of $<1\times10^{-9}$ sec and hence a scale factor of <.15 cm^{-1}. With $T_1=T_2$ and only the ground level populated a crystal 30 cm long would still be required.

Unusually narrow linewidths as well as short relaxation times generally characterize lanthanide ion spectra but energy level splittings usually range from 10-100 cm^{-1}.[40] Some notable exceptions are Dy^{+3} and Er^{+3} in nearly cubic hosts like YA_sO_4 where

energy level splittings can be on the order of 1 cm. Unfortunately, observed linewidths are very broad.

Non-Kramers ions for example, Fe^{+2} (T_1=2 μs)[41] and ions which exhibit Jahn-Teller coupling to the lattice, V^{+3}, ($T_1=1\times10^{-5}$ sec)[42] might be considered but again the inhomogeneous linewidths are very wide. In general, for good conversion efficiencies at moderate conversion distances it is necessary that T_1 be of the same order of magnitude as T_2 and neither T_2 nor T_2^* should be faster than 10^{-7} or 10^{-8} sec. In addition, the bulk of the equilibrium population must be in the ground state implying for NMM wave frequencies liquid helium temperatures. Some other candidate magnetic resonance systems might be Mn^{+2} in $CaWO_4$ co-doped with a fast relaxer like Fe^{+2} or Ho^{+3} doped $YLiF_4$.[43]

V. Resonant Tripling

Because of the material parameter limitations, the paramagnetic spins systems do not appear favorable for efficient (>25%) second harmonic generation. However, the tunability and choice of energy spacing does not preclude higher order harmonic situations such as resonant frequency tripling.

We have studied this problem also in a manner analogous to the resonant doubling system just outlined. The equations and resulting solutions are totally opaque and will not be listed for this reason.

Our findings on the dependence of the third harmonic conversion efficiency versus various material parameters and pump intensity suggest that unlike the case of second harmonic generation in a three-level system for which the harmonic absorption is split out of resonance by the pump, harmonic absorption is split out of resonance by the pump, harmonic absorption is always present and limits the conversion efficiency to about $\sim$ 25%. Further, under conditions of strong conversion into the third harmonic, there is a non-negligible gain for the second harmonic which places some severe restraints on the phase matching system to act as a filter for this work. Because of these features, resonant tripling in general does not appear to be a viable approach if high efficiency is sought.

VI. Nonlinear Semiconductors

In an effort to find materials more suitable for efficient doubling, some thought was given to semiconductor systems. It is well known that the I-V curves of a diode are highly nonlinear with the forward biased situation used in mixer technology and the reverse biased situation used in varactor technology. In the latter case, the nonlinearity arises because of the dependence of the depletion width and hence depletion layer dipole on the applied potential. The nonlinearity is enormous by optical standards but is more distributed and requires conduction paths to transform free space or guided waves into the devices. Out of necessity, this introduces losses so that the best reported doubling efficiency in the NMMW was $\sim$ 10%.[44] Other schemes involving modulation doped heterostructures might be anticipated to be no better although still worthy of investigation.[45]

The primary origin of the optical nonlinearity in bulk semiconductors is the non-parabolicity of the bands. While of modest size in the infrared, the nonlinear coefficients become very large a NMMW frequencies. Even with this increase, the required power for efficient conversion is still large, $\sim$ MW/cm^2 for a conversion $\sim$ 50% in 1 cm.

Highly nonparabolic bands are known to exist in heterostructure systems comprised of, for example, GaAs-$Al_xGa_{1-x}As$ superlattices. Tsu and Esaki[46] were the first to consider optical nonlinearities in a symmetric periodic superlattice. They showed that with a

symmetry breaking DC field, the AC current has a component at 2ω corresponding to doubling wherein the nonlinearity is due to an I-V nonlinearity. More recently Bloss and Friedman[47] and Yuen[48] have both considered third order optical nonlinearities in superlattices and showed that these may be large under suitable conditions, some 100 times larger than in the bulk.

The above three theoretical studies were all based on nonlinear transport properties of carriers located in the lowest subband within the conduction bands. It is also possible to have radiative transitions between subbands and to have optical nonlinearities in analogy with what is seen in normal situations. Orlov has considered a symmetric superlattice and concluded that the third order optical-like nonlinearity may be some six orders of magnitude larger than in the equivalent bulk crystal.[49] The origin of the nonlinearity is in the large optical matrix elements associated with the envelope wave functions of the confined carriers. This is analogous to the situation in the nonlinear polymer MNA.[50]

For symmetry reasons, the lowest order nonlinearity associated with a periodic symmetric potential is restricted to odd harmonic. We have recently shown that asymmetric potentials may be achieved in superlattices with the use of compositional grading and that the lowest order quadratic nonlinearity is estimated to be some two orders of magnitude larger than in bulk samples.[51] Because of practical difficulties in growing very low compositional

gradients, this approach will be most useful in the infrared region and is expected to yield nonlinearities in the NMM region comparable to existing materials.

There are other possiblities for the superlattice case involving charge rearrangement within a potential region, analogous to the varactor case,[45] which have not yet been explained in any detail. These are not radiative transitions based nor nonlinear I-V in nature but rather "loose" dipoles. In the NMM region some power dissipation must occur out of necessity but the magnitude of the loss and the magnitude of the nonlinearity remain to be determined. Clearly, there are other possibilities for efficient doubling in the NMM range and some of these approaches seem worthy of further study.

References

1. T. A. DeTemple, L. A. Bahler, J. Osmundsen, "Semiclassical Theory of Resonant Three-Wave Parametric Interactions: Second Harmonic Generation", Phys. Rev. A. 24, 1950-1964 (1981).

2. K. S. Yngvesson and E. L. Kollberg, Efficient Microwave Second Harmonic Generation and Frequency Conversion in Fe^{+3}-TiO_2", Appl. Phys. Lett. 36, 104-106 (1980).

3. A. M. Clogston, "Susceptibility of the Three-Level Maser", J. Chem. Phys. 4, 271-277 (1958).

4. A. Jęlenski, "The Resonance Conversion of Frequency in Paramagnetic Crystals", Electron. Tech. 3, 127 (1970).

5. R. Boscaino, I. Ciccarillo, C. Cusumano, and M.W.P. Strandberg, "Second-Harmonic Generation and Spin Decoupling in Resonant Two-Level Spin Systems", Phys. Rev. B. 3, 2675-2682 (1971).

6. R. Boscaino, B. Brai, I, Ciccarello, "Spectral Spin Diffusion in Dilute Ruby", Phys. Rev. B. 13, 2798-2804 (1976).

7. K.-H. Steiner, "Interactions Between Electromagnetic Fields and Matter, Pergamon Press & Vieweg, 1973.

8. C. M. Kellington, "Resonant harmonic Generation in Ruby", Phys. Rev. Lett. 9, 57-58 (1962).

9. R. Boscaino, B. Brai, I. Ciccarello and M.W.P. Strandberg, "Effect on Strong Radio-Frequency Field on the Transverse Relaxation Time in Paramagnetic Solids", Phys. Rev. B. 7, 50-53 (1973).

10. W. H. Higa, "Low-Level Microwave Mixing in Ruby", Proc. IEEE, 54, 1453 (1966).

11. E. G. Solov'gev, A. V. Startsev, "Frequency Conversion in a Multi-Level Quantum System", Radio Eng. El. Phys. 13, 1322 (1968).

12. G. Dathe, D. Roth, G. H. Schollmeiir, K. H. Steiner, "Microwave Frequency Doubling in Ruby", IEEE J. Quant. Elec. QE-5, 169 (1969).

13. E. O. Schulz-Dubous, "Theory of Intermodulation and Harmonic Generation in Traveling-Wave Masers", Proc. IEEE. 52, 644 (1964).

14. L. Bahler, "Resonant Second Harmonic Generation: Propagation Study", M.S. Thesis, University of Illinois, Urbana, IL, 1981.

15. C. P. Slichter, Principles of Magnetic Resonance, Springer Verlag, Berlin, Heidelberg, New York (1980).

16. K. S. Yngvesson, "Cr-TiO_2 as an L-Band Maser Material", J. Quan. Elec. 2, 165 (1966).

17. D. L. Carter, "An Ultrasonic Continuous Wave Solid State Push-Pull Maser in the 5 to 6 Millimeter Wavelength Region", J. Appl. Phys. 32, 2541-2542 (1961).

18. S. Forer and L. R. Mo, "CW Millimeter Wave Maser Using Fe^{+3} in TiO_2", J. Appl. Phys. 31, 742-743 (1960).

19. F. Arams and B. Peyton, "Tunable Millimeter Travelling-Wave Maser Operation", Proc. IRE, 50, 1697 (1962).

20. G. I. Lichenberger and J. R. Addision, "F- and x-band Spectroscopy on Fe^{+3} in Rutile", Phys. Rev. 184, 381-382 (1969).

21. P. O. Anderson, E. L. Kollberg, and A. Jelenski, "Extra EPR Spectra of Iron-Doped Rutile", Phys. Rev. B. 8, 4956-4965 (1973).

22. D. L. Carter and A. Okaya, "Electron Paramagnetic Resonance of Fe^{+3} in TiO_2 (Rutile)", Phys. Rev. 118, 1485-1490 (1960).

23. K. S. Yngvesson, private communication.

24. M. Baran, H. Szymczak, J. Wosik, and W. Piekarczyk, "Spin-Lattice Interaction for Fe Ions in TiO_2", Elec. Tech. 6, 185-193 (1973).

25. S. Tanaka, K. Mizushi, and S. Iida, "Electron Spin-Lattice Relaxation of Fe^{+3} Ion in Rutile, J. Phys. Soc. Japan, 49, 1291-1298 (1980).

26. G. J. Lichtenbergen, "Spin-Lattice Relaxation of Fe^{+3} in Rutile for x- and F-band Transitions", Can. J. Phys. 47, 1573-1583 (1969).

27. M. P. Madan, "Spin Lattice Relaxation Time of Fe^{+3} Ion", Can. Phys. 42, 583-594 (1964).

28. A. A. Manenkov and A. M. Prokhorov, and V. A. Milyaev, "Cr^{+++} and Fe^{+++} the Relaxation Time of Single Crystals of Rutile", Sov. Phys. Solid State, 4, 280-283 (1962).

29. M. Alam, S. Chandra and G. R. Hoy, "Hyperfine-Field Fluctuations in Fe^{+3}-Doped TiO_2 Using Mossbauer Effect", Bull. Am. Phys. Soc. 11,

30. M. Alam, S. Chandra, and G. R. Hoy, "Mossbauer Studies of Spin Relaxation of Iron (III) in Titanium Dioxide", Phys. Lett. 22, 26-28 (1966).

31. C. A. Bates, A. Gavaix, P. Steggles, A. Vasson, and S.-M. Vasson, "Non-Resonant Cross-Relaxation and Its Occurrence in Vanadium-Doped Rubies", J. Phys. C.: Solid State Phys. 9, 2413-2427 (1976).

32. C. A. Bates, P. Steggles, A. Vavaix, A.-M. Vasson, and A. Vasson, "Cross Relaxation in Nickel Doped Rubies", J. Phys. Paris, 39, 315-329 (1978).

33. C. A. Bates, A. Vavaix, P. Steggles, A. Vasson, and A.-M. Vasson, "Cross-Relaxation to Fast Relaxing Ions in Alumina", J. Phys. C: Solid State Phys. 8, 2300 (1975).

34. A. G. Redfield, "Nuclear Magnetic Resonance Saturation and Rotary Saturation in Solids", Phys. Rev. 98, 1787-1809 (1955).

35. M.W.P. Strandberg, "Strong-Radio-Frequency-Field Effects in Nuclear Magnetic Resonance and Electron Paramagnetic Resonance", Phys. Rev. B. 6, 747-756 (1972).

36. R. Boscaino and A. Tripo, "Two-Photon Transitions in Spin Systems: Effect of a Resonant Intermediate Level", J. Phys. C: Solid State Phys. 9, L155-L158 (1976).

37. D. A. Bozanic, D. Mergerian, and R. W. Minarik, "Nickel-Doped Rutile as a Spin-Echo Material", J. Appl. Phys. 41, 5041 (1970).

38. D. A. Bozanic, D. Mergerian, and R. W. Minarik, "Spin-Echo Studies of Exchange Effects in Heavily Doped TiO_2: Fe^{+3}", Phys. Rev. Lett. 23, 1212 (1969).

39. D. Shaltiel and W. Tow, "Anistropic Broadening of Linewidth in the Paramagnetic Resonance Spectra of Magnetically Dilute Crystals", Phys. Rev. 124, 1062-1067 (1961).

40. A. Abragam and B. Bleaney, Electron Paramagnetic Resonance of Transition Metal Ions, Clarendon Press, Belfast, (1970) p. 285.

41. C. A. Bates and P. Steggles, "The Jahn-Teller Theory and Calculations of the Relaxation Time and Resonance Lineshape for Fe^{+2} Ions in Al_2O_3, J. Phys. S. Solid State Phys. 8, 2283-2299 (1975).

42. G. M. Zverev, A. M. Prokhorov, and A. K. Shevchenko, "Effect of Vanadium on the Spin Lattice Relaxation of Chromium Doped Rubies", Sov. Phys. Solid State, 4, 2297-2302 (1963).

43. J. Magarino, J. Tuchindler, J.P.D. Haenens, A. Ling , "Sub-millimeter Resonance Spectroscopy of Ho^{+3} in Lithium Yttrium Floride", Phys. Rev. B. 13, 2805-2808 (1976).

44. T. Takada, T. Makimura and M. Ohmori, "Hybrid Intengrated Frequency Doublers and Triplers to 300 and 450 GHz", IEEE Trans. Micro. Theo. and Tech., MTT-28, 966-973 (1980).

45. D. P. Houson, B. Owen and G. T. Wright, "The Space-Charge Varactor", Solid State Elec. 8, 913-921 (1965).

46. R. Tsu and L. Esaki, "Nonlinear Optical Response of Conduction Electrons in a Superlattice", Appl. Phys. Lett. 19, 246-248 (1971).

47. W. L. Bloss and L. Friedman, "Theory of Optical Mixing by Mobile Carriers in Superlattices", Appl. Phys. Lett. 41, 1023-1025 (1982).

48. S. Y. Yuen, "Third-Order Optical Nonlinearity Induced by Effective Mass Gradient in Heterostructures", Appl. Phys. Lett. 42, 331-333 (1983).

49. K. L. Orlov, "Third Harmonic Generation in Semiconductors with a Superlattice", Sov. J. Radiophysics, 19, 1315-1319 (1976).

50. See for example the review by A. F. Garito and K. D. Singer, "Organic Crystals and Polymers - A New Class of Nonlinear Optical Materials", Laser Focus, 59-63, (February 1982).

51. M. K. Gurnick and T. A. DeTemple, "Synthetic Nonlinear Semiconductors", IEEE J. Quan. Elec. (May 1983).

52. R. G. DeVoe and R. G. Brewer, "Experimental Test of the Optical Block Equations for Solids", Phys. Rev. Lett. 50, 1269-1272 (1983).

Personnel Associated with Grant

T. A. DeTemple, Co-principal Investigator

October 1, 1981 - July 20, 1982 - 10%
December 1, 1982 - February 3, 1983 - 25%

J. R. Tucker, Co-principal Investigator

October 1, 1981 - May 20, 1982 - 10%

M. K. Gurnick, Visiting Research Associate

October 1, 1981-September 30, 1982 - 100%

List of Publications

1. "Synthetic Nonlinear Semiconductors", M. K. Gurnick and T. A. DeTemple, IEEE J. Quantum Electron, QE-19, 791-794, (1983).

2. "Resonant Second Harmonic Generation", M. K. Gurnick and T. A. DeTemple, in progress.

3. "Resonant Four-Wave Interactions: Third Harmonic Generation", M. K. Gurnick and T. A. DeTemple, in progress.